A Resonance Raman Spectroelectrochemical Study of the Zn(II) Tetraphenylchlorin Anion

Milton E. Blackwood, Jr., Ching-Yao Lin, Susan R. Cleary, Michael M. McGlashen, and Thomas G. Spiro*

Department of Chemistry, Princeton University, Princeton, New Jersey 08544

Received: July 12, 1996; In Final Form: October 21, 1996[⊗]

Zinc(II) tetraphenylchlorin (ZnTPC) and its π-anion radical have been studied by UV−vis absorption and resonance Raman (RR) spectroscopies. Analyses of the RR spectra were aided by data for the pyrrole-d_8, *meso*-C_{13}, and phenyl-d_{20} isotopomers. Upon formation of the anion, significant frequency shifts are observed in skeletal vibrational modes, while substituent modes remain essentially unshifted. Both frequency upshifts (ν_{37}, ν_{10}, and ν_{19}) and downshifts (ν_2, ν_{11}, and ν_3) occur for the $C_\alpha C_m$ and $C_\beta C_\beta$ stretching modes in the π-anion. Modes involving significant $C_\alpha C_\beta$ stretching motion, ν_4 and ν_{41}, upshift in the anion spectrum. The pattern of vibrational frequency shifts for the anion of ZnTPC is similar to what is observed for the anion of vanadyl tetraphenylporphyrin ((VO)TPP) despite the reduction of a pyrrole ring in TPC. This resemblance is due to the Jahn−Teller distortion in $(VO)TPP^-$, which gives its singly occupied molecular orbital the same bonding pattern as in $ZnTPC^-$.

Introduction

There is extensive interest in understanding the physical properties of π-radical species of both metalloporphyrins and metallochlorins because of the crucial roles they play in biological processes.[1] The π-radicals of metallochlorins are of particular importance because they are formed as transients during the primary events of photosynthesis.[2] To understand the mechanism of photosynthesis, it is necessary to determine how the formation of these radicals alters the structures of metallochlorins. Because of the sensitivity of vibrational frequencies to structural changes, resonance Raman (RR) spectroscopy is an effective tool for studying π-radicals of chromophores. Extensive RR studies are beginning to unravel the structural properties of metalloporphyrin π-radicals.[3] In contrast, with few exceptions,[4] RR studies of metallochlorins have been limited to neutral, ground state species.[5]

Since the lowest unoccupied molecular orbitals (LUMO's, e_g*)[6] in metalloporphyrins are degenerate, the anions and excited states are subject to Jahn−Teller distortions. The nature and extent of this effect have been investigated by RR spectroscopy.[3] The reduction of one of the pyrrole rings in converting metalloporphyrins to metallochlorins lowers their symmetry from D_{4h} to C_{2v}. As a result, the LUMO in metallochlorins is nondegenerate, and thus, a Jahn−Teller distortion is not expected in their anions and excited states. RR studies of the triplet states of metallochlorins have revealed vibrational frequency shift patterns quite different from RR studies of the triplet states of their parent metalloporphyrins. These differences indicate that the structural changes in this excited state of metalloporphyrins and metallochlorins are unique.[3c−e] The limited data on the anions of metallochlorins prevent a similar comparison to be made with the anions of metalloporphyrins.

To extend our knowledge of metallochlorin anions, we have used RR spectroscopy to study Zn(II) tetraphenylporphyrin (ZnTPC), Figure 1, and its monoanion species. A previous study of the Zn(II) octaethylchlorin (ZnOEC) found only small changes in the RR spectrum upon one-electron reduction.[4b] That study was limited to the natural abundance (NA) species. The lack of isotope data makes assignments of features in the Raman spectra of complex molecules difficult and limits the structural information that can be extracted. To successfully assign most spectral features, in addition to the NA species, we have also studied the pyrrole-d_8, *meso*-C_{13}, and phenyl-d_{20} isotopomers of ZnTPC. These results allow us to compare the structural changes observed in the ZnTPC anion to those observed in metalloporphyrins anions.

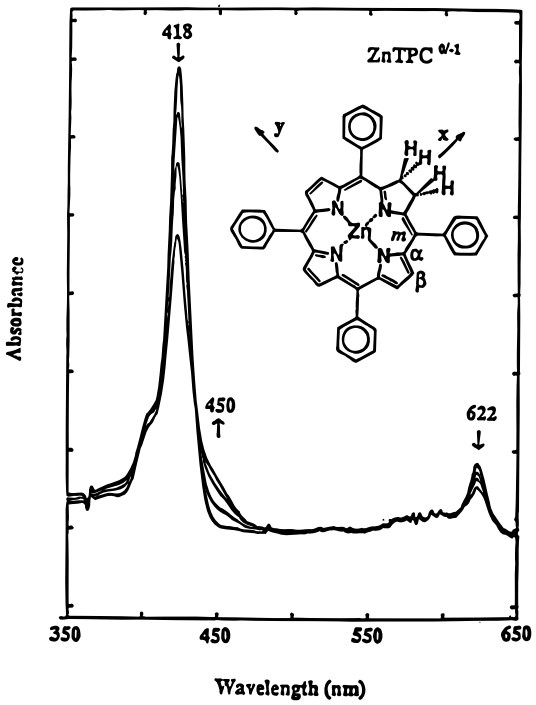

Figure 1. Electronic absorption spectrum of Zn(II) tetraphenylchlorin, ZnTPC, as it is progressively converted (arrows) to its anion radical by electrolysis at −1.5 V vs SCE. The molecular structure and labeling scheme for ZnTPC are shown in the inset.

Experimental Section

Materials. Natural abundance (NA) ZnTPC was purchased from Midcentury Chemical Co. (Posen, IL). To prepare the *meso*-C_{13}, pyrrole-d_8, and phenyl-d_{20} isotopomers of ZnTPC,

* To whom correspondence should be addressed.

[⊗] Abstract published in *Advance ACS Abstracts,* December 15, 1996.

S1089-5639(96)02081-6 CCC: $14.00

the appropriately labeled free base tetraphenylporphyrins (TPP's) were first synthesized according to the method of Lindsey *et al.*[7] The diimide reduction reaction described by Whitlock *et al.*[8] was then used to convert the free base porphyrin to free base chlorin. Zinc(II) was inserted into the chlorin macrocycle using standard procedures.[9] The ZnTPC complexes were purified on 1000 μm silica gel plates using a degassed 1:1 (v:v) mixture of THF and hexane as an eluant. The purifications were all performed in a glovebox under a nitrogen atmosphere (Vacuum Atmosphere Model D1-001-SSD equipped with an He-493 Dri-Train) as ZnTPC in solution is readily oxidized to ZnTPP.

Electrochemistry and Spectroelectrochemistry. All experiments were performed in thoroughly degassed anhydrous DMF (Aldrich). Tetrabutylammonium perchlorate (0.2 M, Fluka) was used as a supporting electrolyte. The electrolyte was dried in a vacuum oven overnight prior to use. All cells were airtight and were assembled under an inert atmosphere. A Princeton Applied Research Model 173 potentiostat was used to control the potential in all experiments.

The cyclic voltammogram of ZnTPC was measured with a standard three-electrode electrochemical cell, using a 1 mm platinum polished working electrode. A saturated calomel electrode (SCE) served as a reference electrode and was isolated from the working compartment by a glass junction with a platinum wire sealed in the tip. The counter electrode was a platinum gauze isolated from the working compartment by a fine glass frit.

UV−vis spectra were recorded with a Hewlett-Packard diode array 8451A spectrophotometer. The absorption spectrum of the ZnTPC radical anion was obtained in an optically transparent thin layer electrochemical (OTTLE) cell that had a 100 mesh platinum gauze working electrode in a 1 mm quartz cell. The reference (SCE) and counter electrodes (a platinum wire) were isolated from the working compartments by fine glass frits. The bulk electrolysis cell used for the RR spectroelectrochemistry was similar to one describe previously.[10] The RR cell allowed continuous sample stirring so that exhaustive electrolysis of the neutral parent could be achieved. All electrolysis experiments were reversible, and there was no evidence for phlorin formation in any of the spectra.

The RR spectra were obtained with 135° backscattering geometry from the bulk electrolysis cell. A Spectra Physics 164 Ar^+ laser provided 457.9 nm excitation. The scattered light was collected and dispersed with a Spex single-stage spectrograph and detected with a liquid nitrogen cooled CCD detector (1024 × 256 EEV, Princeton Instruments).

Results

UV−vis Spectroelectrochemistry. The cyclic voltammogram (CV) of ZnTPC (not shown) exhibits two reversible reduction waves with $E_{1/2}$'s of −1.29 and −1.66 V vs SCE. For the OTTLE experiment (Figure 1) the working electrode was held at −1.5 V vs SCE, and the absorption spectrum was measured every 5 min until no changes were observed. Consistent with results for other tetrapyrrolic π-anions,[6] there is a red shift in the B bands and a bleaching of the Q bands. The presence of isosbestic points at 375 and 430 nm shows that a clean reduction occurred. For all RR experiments 457.9 nm excitation was utilized. Although this wavelength is preresonant with the B bands of neutral ZnTPC, spectra were obtained at sample concentrations of ca. 1 mM. Upon the reduction of ZnTPC, the red shifts of the B bands result in much stronger scattering at this excitation wavelength from the π-anion, and the spectra are uncontaminated by features arising from trace remnants of the neutral parent.

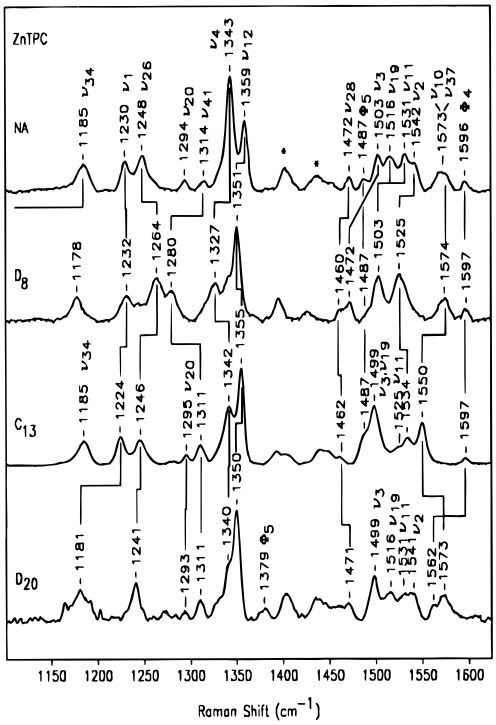

Figure 2. The 457.9 nm excited RR spectra of natural abundance (NA) ZnTPC and its pyrrole-d_8, *meso*-C_{13}, and phenyl-d_{20} isotopomers in DMF. The asterisks indicate solvent bands. Spectral acquisition times were 10 min, and 200 μM slit widths were utilized. The power used to obtain each spectrum was approximately 15 mW (at the sample).

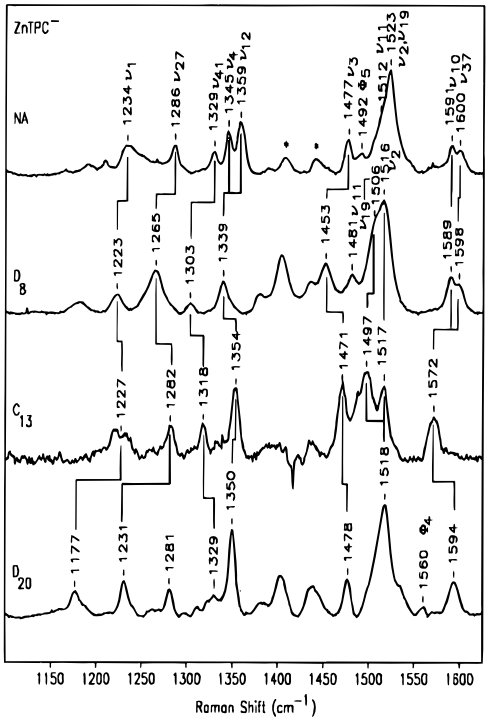

Figure 3. The 457.9 nm excited RR spectra of the anion of natural abundance (NA) ZnTPC and its pyrrole-d_8, *meso*-C_{13}, and phenyl-d_{20} isotopomers in DMF. The anions were prepared by electrolysis of the neutral parent at −1.5 V vs SCE. The asterisks indicate solvent bands. Spectral acquisition times were 10 min and 200 μM slit widths were utilized. The power used to obtain each spectrum was approximately 15 mW (at the sample).

Resonance Raman Spectroscopy. RR spectra for the natural abundance (NA) ZnTPC and its pyrrole-d_8, phenyl-d_{20}, and *meso*-C_{13} isotopomers are shown in Figure 2. Band assignments are based on previous RR studies of metallochlorins. They are

TABLE 1: Neutral and π-Anion Vibrational Frequencies (cm^{-1}) for ZnTPC and Its Isotopomers

vibrational mode	ZnTPC	Δd_8	ΔC_{13}	Δd_{20}	$ZnTPC^-$	Δd_8	ΔC_{13}	Δd_{20}	$\Delta^{0/-}$
$\Phi_4(C_pC_p)$	1596	+1	+1	−34	*b*	*b*	*b*	−36[a]	*b*
$\nu_{37}(C_\alpha C_m)$	1573	+1	−23	0	1600	−2	−28	−6	+27
$\nu_{10}(C_\alpha C_m)$	1573	+1	−23	0	1591	−2	−19	+3	+18
$\nu_2(C_\alpha C_m)(C_\beta C_\beta)$	1542	−17	−8	−1	1523	−7	−6	−5	−19
$\nu_{11}(C_\beta C_\beta)$	1531	−28	−6	0	1512	−31	*b*	*b*	−19
$\nu_{19}(C_\alpha C_m)(C_\beta C_\beta)$	1516	−13	−17	0	1523	−17	−26	−5	+7
$\nu_3(C_\beta C_\beta)$	1503	−31	−4	−4	1477	−24	−6	+1	−26
$\Phi_5(C_pC_p)$	1487	0	0	−110	1492	*b*	*b*	*b*	+5
$\nu_{28}(C_\alpha C_m)(C_\beta C_\beta)$	1472	−12	−10	−1	*b*	*b*	*b*	*b*	*b*
$\nu_{12}(C_\alpha N)(C_\alpha C_\beta)$	1359	−8	−4	−9	1359	−20	−5	−9	0
$\nu_4(C_\alpha C_\beta)(C_\alpha N)$	1343	−16	−1	−3	1345	*b*	*b*	*b*	+2
$\nu_{41}(C_\alpha C_\beta)(C_\alpha N)$	1314	−34	−3	−3	1329	−26	−11	0	+15
$\nu_{20}(C_\alpha C_\beta)(C_\alpha N)$	1294	*b*	+1	−1	*b*	*b*	*b*	*b*	*b*
$\nu_{27}(C_mPh)$	*b*	*b*	*b*	*b*	1286	−21	−4	−55	*b*
$\nu_{26}(C_\alpha C_\beta)(\delta C_\beta H)$	1248	+16	−2	−7	*b*	*b*	*b*	*b*	*b*
$\nu_1(C_mPh)$	1230	+2	−6	−49	1234	−11	−7	−57	+4
$\nu_{34}(\delta C_\beta H)$	1185	*b*	0	*b*	*b*	*b*	*b*	*b*	*b*

[a] From the NA neutral frequency. [b] Not observed.

consistent with those from our previous study of ZnTPC and its triplet excited state,[4c] but the availability of new *meso*-C_{13} isotopomer data permits several new assignments. In addition, ν_3 is reassigned to a peak that was not enhanced at the excitation wavelength used in the previous study. The mode numbering system is based on analogy with the NiTPP normal modes.[11] Vibrational analysis of Ni(II) octaethylchlorin[5i] has indicated that ring reduction does not greatly effect mode composition (except for the reduced $C_\beta C_\beta$ bond). Additional modes become RR active, however, due to the symmetry lowering.

The anions were generated for the RR measurements by reducing the neutral parent at −1.5 V. Spectral features in the anion spectra (Figure 3) are correlated with neutral species features based on similar intensity and isotope shift patterns. The neutral and anion vibrational assignments for ZnTPC are summarized in Table 1.

The Neutral Species. The higher frequency (>1450 cm^{-1}) portion of the spectra (Figure 2) contain $C_\beta C_\beta$ and $C_\alpha C_m$ stretching modes. These modes can be identified via downshifts of Raman peaks upon *meso*-C_{13} or pyrrole-d_8 substitution. The complex band at ∼1573 cm^{-1} contains two $C_\alpha C_m$ stretching modes, ν_{10} and ν_{37}, as judged by large downshifts in the *meso*-C_{13} spectrum. In contrast, the peaks at 1531 and 1503 cm^{-1} are only slightly C_{13} sensitive but undergo large pyrrole-d_8 downshifts and are assigned to the predominately $C_\beta C_\beta$ stretching modes, ν_{11} and ν_3. The other bands in this region, 1542, 1516, and 1472 cm^{-1}, are sensitive to both pyrrole-d_8 and *meso*-C_{13} substitution and assigned to ν_2, ν_{19}, and ν_{28}, which are mixtures of $C_\beta C_\beta$ and $C_\alpha C_m$ stretching. The two remaining bands in this region, 1596 and 1487 cm^{-1}, shift strongly in the phenyl-d_{20} spectrum and are assigned to the phenyl modes, Φ_4 and Φ_5.

In the 1100−1400 cm^{-1} region, the bands at 1185, 1230, 1314, 1343, and 1359 cm^{-1} are assigned to ν_{34}, ν_{11}, ν_{41}, ν_4, and ν_{12} as in our previous study.[4c] Two new features are now identified, ν_{26} (1248 cm^{-1}) and ν_{20} (1294 cm^{-1}), on the basis of the similarity of their isotope shift patterns to the corresponding modes in NiTPP.[11] The ν_{26} mode is a mixture of $C_\alpha C_\beta$ stretching and $C_\beta H$ bending motions while ν_{20} is a mixture of $C_\alpha N$ and $C_\alpha C_\beta$ stretching motions.[11]

The π-Anion. Large frequency shifts are seen in the $C_\alpha C_m$ and $C_\beta C_\beta$ stretching modes in the anion spectrum of ZnTPC (Figure 3). Both $C_\alpha C_m$ modes, ν_{10} and ν_{37}, are now clearly resolved, 1600 and 1591 cm^{-1}, and are at significantly higher frequencies than in the neutral species. Their C_{13} sensitivities are essentially unaltered. Likewise, the $C_\beta C_\beta$ modes, ν_3 and ν_{11}, have nearly the same d_8 sensitivities as in the neutral spectrum, but their frequencies are significantly lower in the anion, 1512 and 1477 cm^{-1}. The mixed $C_\alpha C_m$ and $C_\beta C_\beta$ modes, ν_2 and ν_{19}, are overlapped in the intense peak at 1523 cm^{-1} but are resolved in the pyrrole-d_8 and *meso*-C_{13} spectra. ν_2 shifts down but ν_{19} shifts up upon anion formation. The remaining mixed mode, ν_{28}, is not seen in the anion spectrum.

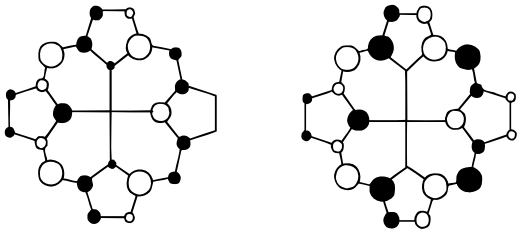

Figure 4. Illustration of the LUMO's for metallochlorins and metalloporphyrins adapted from ref 12.

In the 1100−1450 cm^{-1} region, ν_1,ν_4, and ν_{12} are all found at essentially the same frequencies as in the neutral species, but ν_{41} upshifts by 15 cm^{-1}. The remaining modes in this region of the neutral species are not seen in the anion spectrum but a new peak at 1286 cm^{-1} is assigned to ν_{27} on the basis of its frequency and isotope shift pattern.[11] Like ν_1, this mode is mainly C_m−Ph stretching in character and is strongly d_{20} sensitive. A band at 1281 cm^{-1} in the d_{20} spectrum remains unassigned.

There are no significant frequency shifts in the phenyl modes, Φ_4 and Φ_5. The position of Φ_4 is obscured by overlap with ν_{37} in the natural abundance spectrum, but it is found at 1560 cm^{-1} in the d_{20} spectrum, essentially the same position as in the neutral species d_{20} spectrum.

Discussion

The mode frequency shifts upon anion formation (Table 1) can be understood with reference to the bonding pattern of the ZnTPC LUMO (Figure 4),[12] into which the extra electron is placed. The coefficients are largest on the pyrrole rings adjacent to the reduced ring and on the distant C_m atoms. The orbital is antibonding with respect to the $C_\beta C_\beta$ bonds on the adjacent pyrroles, accounting for the downshifts (−19 and −26 cm^{-1}) in the $C_\beta C_\beta$ modes ν_{11} and ν_3, and it is bonding with respect to the $C_\alpha C_\beta$ bonds, accounting for the upshift in ν_{41}. Both ν_{41} and ν_4 are combinations of $C_\alpha C_\beta$ and $C_\alpha N$ stretching, but ν_4 shifts very little (+2 cm^{-1}) probably because it has more $C_\alpha N$

TABLE 2: Vibrational Frequency Shifts (cm^{-1}) in the Anions of ZnTPC and VO(TPP)

mode	ZnTPC	(VO)TPP[a]	mode	ZnTPC	(VO)TPP[a]
ν_{37}	+27	*b*	ν_3	−26	*b*
ν_{10}	+18	−11	ν_4	+2	+8
ν_2	−19	−8	ν_{41}	+15	*b*
ν_{11}	−19	−29	ν_1	+4	−4
ν_{19}	+7	+27			

[a] From ref 3l. [b] Not observed.

character, and the $C_\alpha N$ interactions are mainly antibonding (Figure 4). The $C_\alpha C_m$ modes, ν_{37} and ν_{10}, shift up strongly (+27 and +18 cm^{-1}), implying that they mainly involve the set of $C_\alpha C_m$ bonds for which the LUMO is bonding, i.e., the bonds adjacent to the reduced ring and the ring across from the reduced ring. No doubt these bonds also contribute to ν_{19}, which shifts up somewhat (+7 cm^{-1}). ν_{19} is a mixture of $C_\alpha C_m$ and $C_\beta C_\beta$ stretching, as evidenced by sensitivity to both ^{13}C and d_8 substitution (Table 1). Likewise, ν_2 is a mixture of these coordinates but has more $C_\beta C_\beta$ character and shifts down (−18 cm^{-1}) in the anion.

Interestingly, this shift pattern is similar to that seen for the porphyrin anion in $(VO)TPP^-$ (Table 2).[3l] The $C_\beta C_\beta$ mode ν_{11} shifts down strongly (−29 cm^{-1}) while the $C_\alpha C_m$ mode ν_{19} shifts up strongly, +27 cm^{-1}. (ν_{19} changes composition in $(VO)TPP^-$, becoming mainly $C_\alpha C_m$ in character, with no d_8 sensitivity.) The pattern deviates somewhat from $ZnTPC^-$, since ν_{10} shifts down (−11 cm^{-1}), not up, while ν_2 shifts less (−8 cm^{-1}) than in $ZnTPC^-$. ν_{41} is not seen for $(VO)TPP^-$, but ν_4 takes over about half (+8 cm^{-1}) of the ν_{41} upshift seen in $ZnTPC^-$.

The similarity ($C_\alpha C_m$ upshift, $C_\beta C_\beta$ downshift) is surprising, since VO(TPP) has degenerate LUMO's, while the degeneracy is completely removed in ZnTPC by the pyrrole reduction. However, the $VO(TPP)^-$ degeneracy is lifted by a B_{1g} Jahn−Teller distortion, which has been shown to account qualitatively for the RR spectral shifts.[3l] The result is stabilization of the b_{1g} LUMO, whose orbital pattern (Figure 4) is strikingly similar to that of the b_1 LUMO in ZnTPC. Thus, the electronic structure of $ZnTPC^-$ strongly resembles that of $(VO)TPP^-$, despite the drastic chemical difference, due to the workings of the Jahn−Teller effect in the porphyrin anion.

Acknowledgment. This work was supported by DOE Grant DE-FG02-93ER-14403.

References and Notes

(1) Frew, J. E.; Jones, P. *Adv. Inorg. Bioinorg. Mech.* **1984**, *3*, 175−212.

(2) Scheer, H., Ed. *Chlorophylls*; CRC: Boca Raton, FL, 1991.

(3) (a) Atamian, M.; Donohoe, R. J.; Lindsey, J. S.; Bocian, D. F. *J. Phys. Chem.* **1989**, *159*, 347. (b) Reed, R. A.; Purello, R.; Prendergast, K.; Spiro, T. G. *J. Phys. Chem.* **1991**, *95*, 9720. (c) Procyk, A. D.; Bocian, D. F. *Annu. Rev. Phys. Chem.* **1992**, *43*, 465. (d) Perng, J.; Bocian, D. F. *J. Phys. Chem.* **1992**, *96*, 4804. (e) Kumble, R.; Hu, S.; Loppnow, G. R.; Vitols, S. E.; Spiro, T. G. *J. Phys. Chem.* **1993**, *97*, 10521−10523. (f) Sato, S.; Kitagawa, T. *Appl. Phys. B* **1994**, *59*, 415. (g) Kreszowski, D. H.; Deinum, G.; Babcock, G. T. *J. Am. Chem. Soc.* **1994**, *116*, 7463. (h) Kumble, R.; Loppnow, G. R.; Hu, S.; Mukherjee, A.; Thompson, M. A.; Spiro, T. G. *J. Phys. Chem.* **1995**, *99*, 5809−5816. (i) Hu, S.; Lin, C.-Y.; Blackwood Jr., M. E.; Mukherjee, A.; Spiro, T. G. *J. Phys. Chem.* **1995**, *99*, 9694. (j) Sato, S.; Aoyagi, K.; Haya, T.; Kitagawa, T. *J. Phys. Chem.* **1995**, *99*, 7766−7775. (k) Vitols, S. E.; Kumble, R.; Blackwood Jr., M. E.; Roman, J. S.; Spiro, T. G. *J. Phys. Chem*, **1996**, *100*, 4180. (l) Lin, C.-Y.; Spiro, T. G. *Inorg. Chem.* **1996**, *35*, 5237−5243.

(4) (a) Nishizawa, E.; Hashimoto, H.; Koyama, Y. *Chem. Phys. Lett.* **1989**, *164* (2, 3), 155. (b) Perng, J.; Bocian, D. F. *J. Phys. Chem.* **1992**, *96*, 10234. (c) Vitols, S. E.; Terashita, S.; Blackwood Jr., M. E.; Kumble, R.; Ozaki, Y.; Spiro, T. G. *J. Phys. Chem.* **1995**, *99*, 7246. (d) de Paula, J. C.; Walters, V. A.; Jackson, B. A.; Cardozo, K. *J. Phys. Chem.* **1995**, *99*, 4373. (e) Blackwood Jr., M. E.; Kumble, R.; Spiro, T. G. *J. Phys. Chem.* **1996**, *100*, 18037.

(5) (a) Andersson, L. A.; Loehr, T. M.; Sotiriou, C.; Wu, W.; Chang, C. K. *J. Am. Chem. Soc.* **1986**, *108*, 2908. (b) Schick, G. A.; Bocian, D. F. *Biochim. Biophys. Acta* **1987**, *895*, 127. (c) Salehi, A.; Oertling, W. A.; Fonda, F. N.; Babcock, G. T.; Chang, C. K. *Photochem. Photobiol.* **1988**, *48* (4), 525. (d) Boldt, N. J.; Donohoe, R. J.; Birge, R. R.; Bocian, D. F. *J. Am. Chem. Soc.* **1987**, *109*, 2284. (e) Donohoe, R. J.; Atamian, M.; Bocian, D. F. *J. Phys. Chem.* **1989**, *93*, 2244. (f) Andersson, L. A.; Loehr, T. M.; Thompson, R. G.; Strauss, S. H. *Inorg. Chem.* **1990**, *29*, 2142. (g) Fonda, H. F.; Oertling, W. A.; Salehi, A.; Chang, C. K.; Babcock, G. T. *J. Am. Chem. Soc.* **1990**, *112*, 9497. (h) Song, O.-K.; Ha, J.-S.; Yoon, M.; Kim, D. *J. Raman Spectrosc.* **1990**, *21*, 645. (i) Prendergast, K.; Spiro T. G. *J. Phys. Chem.* **1991**, 95, 1555. (j) Procyk, A. D.; Kim, Y.; Schmidt, E.; Fonda, H. N.; Chang, C. K.; Babcock, G. T.; Bocian, D. F. *J. Am. Chem. Soc.* **1992**, *114*, 6539.

(6) Gouterman, M. Physical Chemistry, Part A. In *The Porphyrins*; Dolphin, D., Ed.; Academic Press: New York, 1978; Vol. III.

(7) (a) Lindsey, J. S.; Hsu, H. C.; Schreiman, I. C. *Tetrahedron Lett.* **1986**, *27*, 4969. (b) Lindsey, J. S.; Schreiman, I. C.; Kearney, P. C.; Marguerittaz, A. M. *J. Org. Chem.* **1987**, *52*, 827.

(8) Whitlock, H. W., Jr.; Hanauser, R.; Oester, M. Y.; Bower, B. K. *J. Am.Chem. Soc.* **1976**, *41*, 3857−3860.

(9) Fuhrhop, J.; Smith, K. M. In *Porphyrins and Metalloporphyrins*; Smith, K. M., Ed.; Elsevier: New York, 1976; p 798.

(10) Czernuszewicz, R. S.; Macor, K. A. *J. Raman Spectrosc.* **1988**, *19*, 553.

(11) Li, X.-Y.; Czernuszewicz, R. S.; Kincaid, J. R.; Su, Y. O.; Spiro, T. G. *J. Phys. Chem.* **1990**, *94*, 31.

(12) Sekino, H.; Kobayoshi, H. *J. Chem. Phys.* **1987**, *86* (9), 5045.